DOI: 10.1002/ejoc.201000375

Dynamics and Hydration Properties of Small Antifreeze-Like Glycopeptides Containing Non-Natural Amino Acids

Francisco Corzana,*[a] Jesús H. Busto,[a] Marisa García de Luis,[a] Alberto Fernández-Tejada,[a] Fernando Rodríguez,[a] Jesús Jiménez-Barbero,[b] Alberto Avenoza,[a] and Jesús M. Peregrina*[a]

Keywords: Glycopeptides / Conformation analysis / NMR spectroscopy / Molecular dynamics

Novel studies on the synthesis and conformation in aqueous solution of three antifreeze-like glycopeptides containing the sequence Xaa(α-GalNAc)-Ala-Ala, with Xaa being threonine (Thr) or the non-natural amino acids α-methylserine (MeSer) or α-methylthreonine (MeThr), are reported. The study has combined NMR experiments with molecular dynamics simulations. Whereas the Thr derivative is rather rigid in solution and exhibits an extended conformation for the backbone, the non-natural glycopeptides are fairly flexible and show random coil structures for the peptide sequence. On the other hand, only those glycopeptides with a methyl group at Cβ of the underlying amino acid show perpendicular orientation of the sugar with respect to the peptide moiety. This structural feature, together with the rigidity of the Thr-containing glycopeptide, makes this system unique to structure the water molecules of its first hydration shell. In addition, despite its chemical similarity, the different observed conformational behaviors of all these molecules, as well as the differences in their dynamics and hydration properties, make them suitable systems to shed light on the key factors that govern antifreeze activity.

Introduction

Antifreeze glycoproteins (AFGPs) allow polar fishes to survive in seas where the temperature is subzero by depressing the freezing temperature of the blood without increasing osmotic pressure.[1] These versatile properties have attracted significant interest for their possible applications, such as protection of blood platelets and human organs at low temperatures,[2] increase in the effectiveness of the destruction of malignant tumors in cryosurgery,[3] and improvement in the smooth texture of frozen foods.[4]

The primary structure of these AFGPs consists of repeating tripeptide units, $(Thr\text{-}Ala\text{-}Ala)_n$, whose Thr residue is glycosylated with a β-D-galactopyranosyl-(1–3)-α-D-*N*-acetylgalactosamine disaccharide, abbreviated as β-Gal-(1–3)-α-GalNAc. Recently, Nishimura and co-workers reported a paramount work providing critical structure–activity data to understand the mechanism of ice growth inhibition and to rationalize the design of AFGP mimics.[5] On the other hand, the synthesis of different glycosylated analogues with the $[Thr(\alpha\text{-}GalNAc)\text{-}Ala\text{-}Ala]_n$ sequence has been reported, which exhibited significant antifreeze and ice structuring activities, even though they only contain monosaccharide moieties.[6] In a parallel manner, a new glycoprotein from jellyfish has been isolated and its structure elucidated. It contains unique tandem repeats of eight amino acids, containing the Thr-Ala-Ala tripeptide sequence, with Thr glycosylated with α-GalNAc. In this case, the authors mentioned that an antifreeze function is expected for this glycoprotein.[7]

Therefore, many attempts have been made to characterize the structures of AFGPs in solution and to elucidate their mechanism of action. Nishimura and co-workers identified three elements as key features for their activity: the *N*-acetyl group of α-GalNAc, the α-configuration of the glycoside, and the β-methyl group on the Thr moiety.[5] These findings can help to improve the design of new AFGP mimics. In addition, the authors proposed a 3D model for the physiological action of AFGPs, similar to that previously suggested by the Bush and Feeney[8a] and Lane[8b] groups. The structure consists of an extended, left-handed threefold helix of polyproline II type (PPII). This special distribution exhibits all sugar moieties on one side of the helix, allowing direct interaction of the water molecules with the hydroxy groups of the sugar moiety and thus blocking the growth of ice crystals. In this context, a recent study[9] indicates that the α-helical conformation of the AFGPs could also increase at the ice/water interface.

On the other hand, studies on C-linked AFGP analogs[10] stated that not only the changes in the backbone conforma-

[a] Departamento de Química, Universidad de La Rioja, UA-CSIC,
26006 Logroño, Spain
Fax: +34-941299621
E-mail: francisco.corzana@unirioja.es
jesusmanuel.peregrina@unirioja.es
[b] Centro de Investigaciones Biológicas (CSIC), Ramiro Maeztu 9, 28040 Madrid, Spain

Supporting information for this article is available on the WWW under http://dx.doi.org/10.1002/ejoc.201000375.

tion, but also the spatial relationship between the carbohydrate moiety and the peptide backbone could play a key role in the activity of these molecules. The authors concluded that the antifreeze activity could be related to the facility of these molecules to form hydrophobic pockets between the sugar and the peptide moieties. In addition, these authors emphasized the importance of additional studies to elucidate the role of hydration in glycopeptides and its subsequent effects on the conformation and activity in real biological systems.[11] Despite these reports, at the present moment, and to the best of our knowledge, the actual role of both hydration and hydrophobicity on the mechanism of action of AFGPs remains to be elucidated. In fact, different authors have pointed out that the effect of replacement of Thr and Ala residues in the Thr-Ala-Ala sequence of AFGPs would be highly informative.[1a]

In this context, it is important to note that the lack of a low-cost-synthesis of pure samples of AFGPs has been identified as a limiting factor for more extensive studies on AFGPs for commercial and academic applications.[12] Therefore, and within this topic, we have decided to exploit the known peculiarity of certain non-natural Cα-substituted α-amino acids[13] to stabilize helical conformations,[14] particularly α-methylserine (MeSer) and α-methylthreonine (MeThr). Moreover, as we have recently described,[15] these noncoded amino acids show peculiar relative orientations between the carbohydrate moiety and the peptide backbone, which could affect both the formation of hydrophobic pockets and the hydration shell of the glycopeptides.

On this basis, we herein report the synthesis and conformational analysis, in aqueous solution, of different model glycopeptides with the Xaa*-Ala-Ala sequence, where Xaa = Thr or non-natural MeSer/MeThr (Figure 1). In all cases, the carbohydrate moiety is represented by an α-D-*N*-acetylgalactosamine (* = α-GalNAc) unit, whereas the amino and carboxylic functional groups have been transformed into amides to simulate the peptide backbone. The glycopeptide derived from the natural sequence Thr-Ala-Ala has also been studied for comparative purposes.

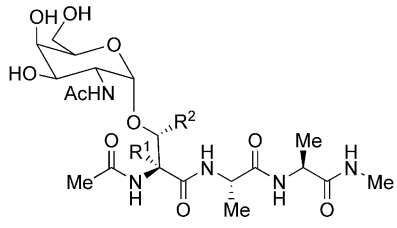

R^1 = H, R^2 = Me, **1**
R^1 = Me, R^2 = H, **2**
R^1 = Me, R^2 = Me, **3**

Figure 1. Antifreeze-like glycopeptides studied in this work.

In particular, NOE-based distance information as well as coupling constants have been interpreted with the assistance of molecular dynamics (MD) simulations. It is important to note that, from a chemical viewpoint, not only is the synthesis of the non-natural target compounds challenging, as the α-amino acid derivatives bear quaternary carbon atoms, but the conformational analysis is also far from trivial. In fact, the absence of the Hα atom in these non-natural amino acids implicates the lack of some key NOE signals and coupling constants, which are pivotal elements to elucidate the existing conformations.

Results and Discussion

Synthesis

As a key example, Scheme 1 shows the synthesis of glycopeptide **2**. The rest of the molecules were synthesized as described in the Supporting Information by following similar methodology. The synthesis started from MeSer derivative **4**, whose carboxylic acid group was protected as a methyl ester function and the amino group as a *tert*-butyloxycarbonyl (Boc) carbamate. Treatment of **4** with 3,4,6-tri-*O*-benzyl-2-nitrogalactal, following the procedure described by Schmidt and co-workers,[16] gave α-linked 2-nitroglycoside **5** in good yield. The reduction of the nitro group by hydrogenation of **5** with nickel Raney (T4) followed by subsequent acetylation of the amino group with acetic anhydride (Ac_2O) and pyridine (Py) led to *N*-acetylated glycoside **6**. Further hydrolysis of the methyl ester with $LiOH·H_2O$ gave corresponding acid **7** in an almost quantitative manner (97%). This compound was then treated with dipeptide **8** and *N*,*N*,*N*′,*N*′-tetramethyl-*O*-(benzotriazol-1-yl)uroniumtetrafluoroborate (TBTU) as a coupling agent in the presence of diisopropylethylamine (DIEA) as a base to give *N*-Boc protected glycopeptide **9** in excellent yield. Deprotection of the amino group and its further acetylation led to intermediate **10**. Finally, purification of compound **10** by column chromatography on silica gel and subsequent hydrogenolysis of the benzyl groups of the sugar moieties with H_2 and Pd/C gave desired glycopeptide **2** derived from MeSer. This compound was purified by reverse-phase HPLC (Scheme 1).

Conformational Study of the Glycopeptides

The clues for dubbing the torsional angles and the atomic labeling used herein are shown in Figure 2.

In a first step, full assignment of the ^1H NMR spectroscopic resonances in all of the compounds was carried out by using standard COSY and HSQC experiments (see Supporting Information). As a next step, a detailed NMR-based structural study of the different glycopeptides was performed. NMR spectroscopic data for derivatives **1**–**3** were recorded at pH 5.5. To analyze the preferred orientations around both the peptide and glycosidic linkages, NOEs were measured by using 2D NOESY in H_2O/D_2O (9:1) and selective 1D NOE in D_2O experiments (Figure 3 and Supporting Information). The key inter-proton distances were derived from the corresponding NOE build-up

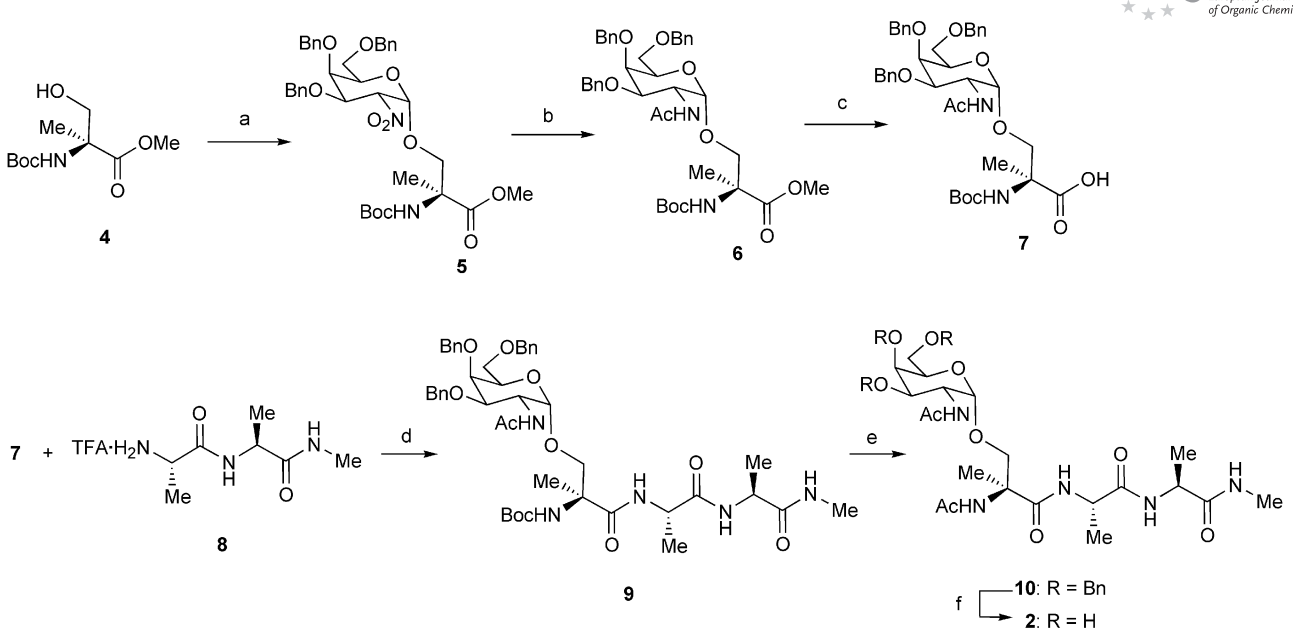

Scheme 1. Synthesis of glycopeptide **2**. Reagents and conditions: (a) 3,4,6-Tri-*O*-benzyl-2-nitrogalactal, *t*BuOK, THF, 25 °C, 12 h, 67%. (b) i. H_2/Ni Raney (T4), EtOH/ethyl acetate (4:1), 25 °C, 4 h; ii. Ac_2O/Py (1:2), 25 °C, 3 h, 41% overall yield. (c) LiOH·H_2O, MeOH/H_2O (4:1), 25 °C, 24 h, 97%. (d) TBTU, DIEA, CH_3CN, 25 °C, 12 h, 97%. (e) i. TFA/CH_2Cl_2 (1:1), 0 to 25 °C, 3.5 h; ii. Ac_2O/Py (1:2), 25 °C, 3 h, 43% overall yield. (f) H_2, Pd/C, MeOH/ethyl acetate (4:1), 25 °C, 12 h, 95%.

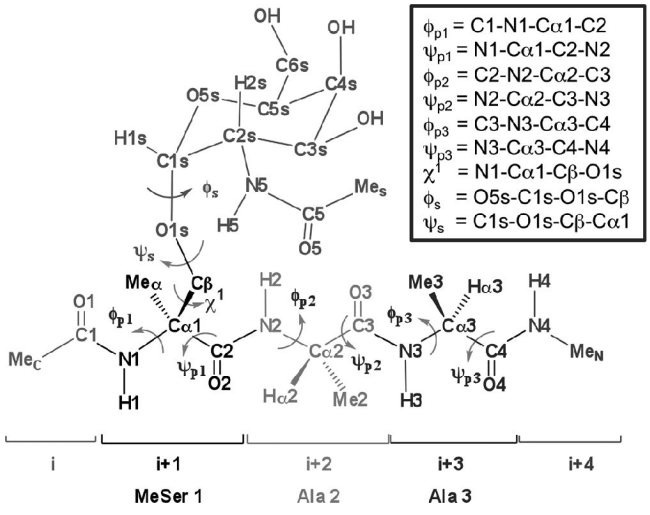

Figure 2. Torsional angles and atom labeling for compound **2**. The same definitions were used for all molecules studied herein.

curves (Figure 3a) by employing the ISPA approximation.[17] These values, together with the H,H homonuclear coupling constants, are represented in Table 1.

The weak or almost absent NH-NH (*i*, *i* + 1) NOE contacts observed in glycopeptide **1** suggests an extended conformation for the backbone of this molecule (Figure 3b). On the contrary, the medium NOE contact between consecutive Hα-NH groups, together with the medium NH-NH (*i*, *i* + 1) ones, detected in derivatives **2** and **3**, suggest the coexistence of both extended and helix-like conformations for the backbone of these molecules (Figure 3c and Supporting Information).[18] Interestingly, the characteristic NOE between NH5 and NH1 previously detected in different Thr-derived glycopeptides[19] was also evidenced in compound **1**.

In order to get a representative ensemble of the conformations present in solution for glycopeptides **1**–**3**, we ran extensive MD simulations in explicit water, including all the NOE-derived distances and ^3J data as time-averaged restraints (MD-tar).[20] Results from these simulations showed close agreement, in numerical terms, between the distances and ^3J values found in the refined models and those extracted from the experimental data (Table 1). Figure 4 shows the superimposition of 10 conformers randomly taken from the MD-tar simulations for each glycopeptide.

Two important conclusions can be drawn from the examination of Figure 4. Firstly, glycopeptide **1** is the most rigid molecule in water solution, with a small RMSD value around 1 Å. Secondly, the backbone of this molecule mainly adopts an extended conformation. In contrast, glycopeptides **2** and **3** are rather flexible and exhibit a random coil conformation for the backbone.

Cluster analysis of the MD simulations revealed that the three residues of glycopeptide **1** simultaneously exhibited ϕ_{pi}/ψ_{pi} typical values of extended conformations for about 80% of the total trajectory time. In particular, the PPII structure was present for about 40% of the total trajectory time. In contrast, the extended conformations were rarely populated by the residues of glycopeptides **2** and **3**. In the later cases, a random-coil distribution was also exhibited by the peptide backbone. Nevertheless, it is important to note that small populations of the two possible type I β-turns

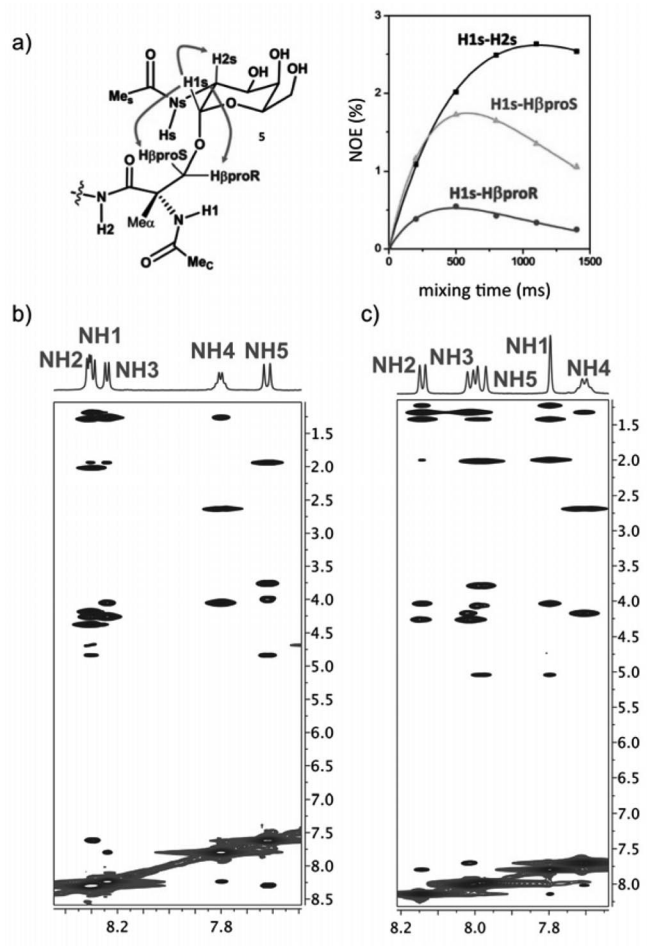

Figure 3. (a) Example of NOE build-up curves corresponding to the anomeric proton of glycopeptide **2**; (b) section of the 800 ms NOESY spectra (400 MHz) of compound **1** in H_2O/D_2O (9:1) at 20 °C showing amide–aliphatic cross-peaks; (c) section of the 800 ms NOESY spectra (400 MHz) of compound **3** in H_2O/D_2O (9:1) at 20 °C showing amide–aliphatic cross-peaks.

Table 1. Comparison of the experimental (NMR) and simulated (MD-tar) distances [Å] and ^3J couplings [Hz] for compound **2**.

	Expt.	MD-tar
NH1–NH2	–[a]	2.1
NH2–NH3	≥3.5	3.3
NH3–NH4	3.2	2.9
NH1–Hβ$_{proS}$	3.0	2.9
NH1–Hβ$_{proR}$	3.0	2.9
NH2–Hβ$_{proS}$	3.5	3.4
NH2–Hβ$_{proR}$	2.9	3.0
H1s–Hβ$_{proS}$	2.4	2.3
H1s–Hβ$_{proR}$	2.8	2.6
NH2–Hα2	2.8	2.8
NH3–Hα2	2.4	2.5
NH4–Hα3	2.3	2.5
NH4-Meα	4.5	5.0
$^3J_{NH2,Hα2}$	5.6	5.2[b]
$^3J_{NH3,Hα3}$	5.8	5.7[b]
$^3J_{NH5,H2s}$	8.9	9.4[b]

[a] Not determined due to signal overlap. [b] Estimated by using the Karplus equation given in reference.[30a]

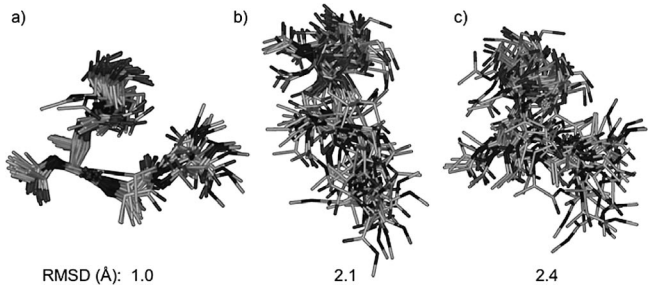

Figure 4. Calculated ensembles obtained from the MD-tar simulations in explicit water for glycopeptides **1** (a), **2** (b), and **3** (c). The numbers indicate the RMSDs for heavy-atom superimposition with respect to the average structure of the trajectory.

were detected for glycopeptides **2** and **3** (Figure 5): one between O1···H3-N (β-turn a) and another one involving O2···H4-N atoms (β-turn b).

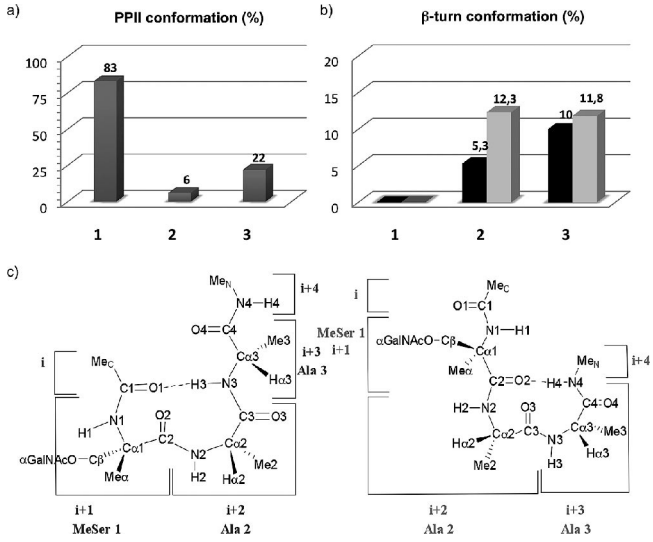

Figure 5. (a, b) Population of the significant conformations obtained from the MD-tar simulations in explicit water for the backbone of the glycopeptides. In (b), the population of type I β-turns a and b is represented in black and grey, respectively. (c) ChemDraw representation of the type I β-turn a (left) and type I β-turn b (right) present in compound **2**.

Figure 6 shows the structural properties of one of the β-turns in compound **2**. This structure is characterized by a weak NOE contact between NH4 and the α methyl group of the MeSer residue.

As far as the lateral chain (χ^1 torsion angle) is concerned, the simulations suggest that the rotation around χ^1 in glycopeptide **1** is very restricted, showing only values close to 60° (Figure 7a). This result is in agreement with the small value of $^3J_{Hα,Hβ}$ (2.5 Hz) experimentally observed for the Thr residue of derivative **1**.[21] In sharp contrast, the lateral chain of the MeSer- and MeThr-containing glycopeptides (compounds **2** and **3**, respectively) are rather flexible, showing a significant population of each of the three possible staggered conformations for this torsion angle. As previously

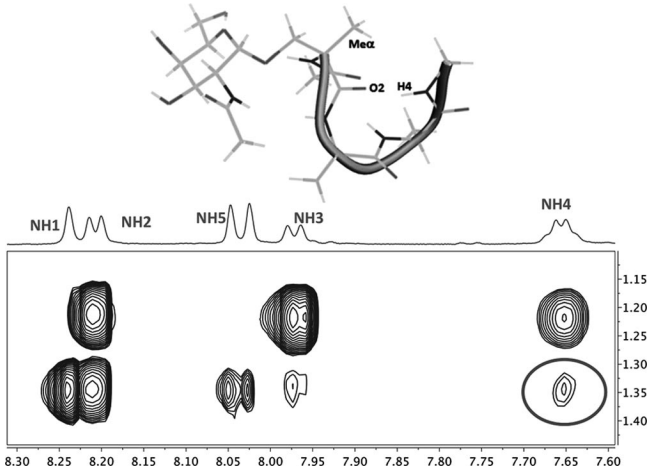

Figure 6. 3D representation of the type I β-turn b observed in compound **2** and section of the 800 ms NOESY spectra (400 MHz) of compound **2** in H_2O/D_2O (9:1) at 20 °C showing amide–aliphatic cross-peaks. The weak NOE contact (grey circle) between NH4 and the α methyl group of the MeSer residue of compound **2** corroborates the existence of this β-turn.

reported by us for other glycopeptides containing the non-natural MeThr residue,[15d] the MD simulations showed a preference for the *anti* conformation (χ^1 close to 180).

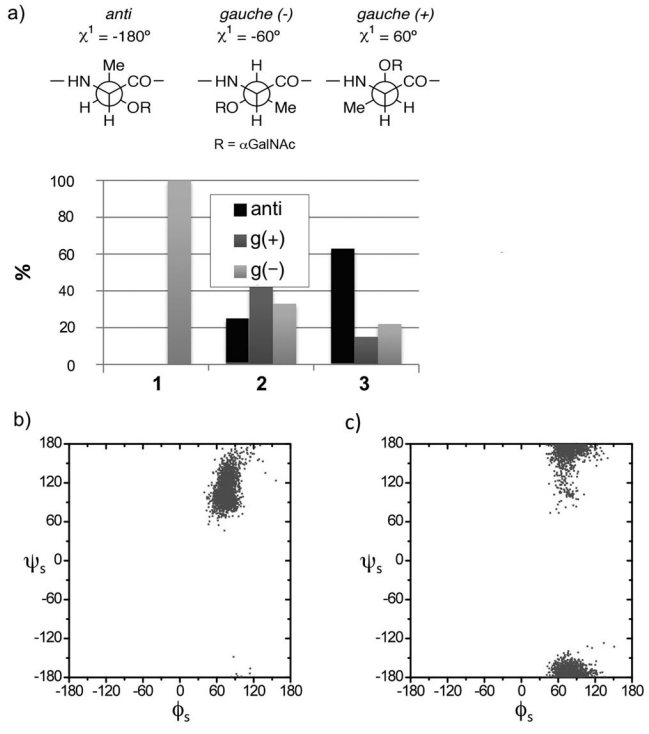

Figure 7. (a) Distribution for the lateral chain (χ^1) obtained from the MD-tar simulations for the three glycopeptides. The Newman projection of the lateral chain of derivative **1** is shown; (b) distribution of the glycosidic linkage (ϕ_s/ψ_s) of compound **1** obtained from the MD-tar simulations; (c) distribution of the glycosidic linkage (ϕ_s/ψ_s) of compound **2** obtained from the MD-tar simulations.

Concerning the glycosidic linkage, the ϕ_s dihedral angle was found to be rather rigid for all compounds (Figure 7b,c), exhibiting values around 60°, in accordance with the *exo*-anomeric effect.[22] However, the glycopeptides with a Me group at Cβ, that is, compounds **1** and **3**, showed a markedly different behavior in terms of the ψ_s (Figure 7b) angles in comparison to the MeSer-containing glycopeptide (compound **2**). In fact, for derivatives **1** and **3** (see Figure 7b and Supporting Information), this angle showed well-defined values around 120–140°, resulting in an eclipsed conformation for the Hβ-Cβ and O1-C1 bonds. Curiously, this eclipsed conformer avoids repulsions between the methyl group at Cβ and the carbohydrate moiety (endocyclic oxygen), which would be present when the ψ_s angle is close to 180°.[19] The different ψ_s values in Thr/Ser-derived glycopeptides allow the carbohydrate moiety to adopt completely distinct orientations. Thus, in compound **1**, the carbohydrate is almost perpendicular to the peptide backbone (Figure 4). As a consequence, the *N*-acetyl group of the carbohydrate in this molecule is in close proximity to the peptide backbone, which favors the existence of a weak hydrogen bond between the carbonyl group of the amino acid (O2) and the NH5 corresponding to NHAc group of the α-GalNAc (Figure 8a). Although the eclipsed conformation was also observed in glycopeptide **3**, this hydrogen bond was rarely populated in this molecule as a result of the inappropriate orientation of its lateral chain. On the other hand, as also reported in the literature, the existence of this hydrogen bond is negligible in solution for Ser-derived glycopeptides.[23]

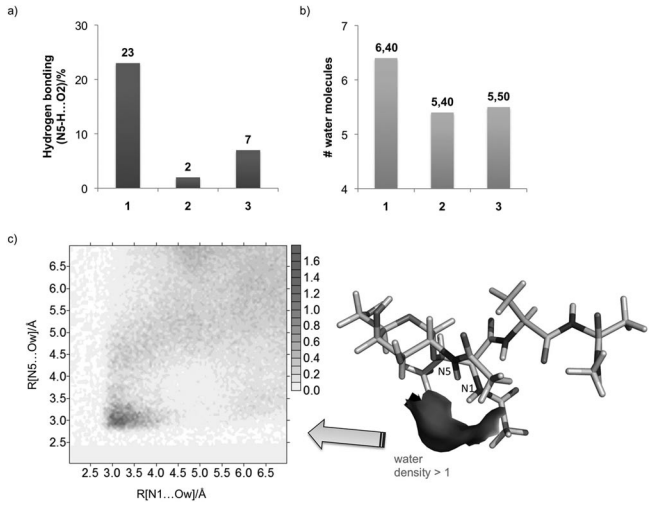

Figure 8. (a) Population of the hydrogen bond between N5-H···O2 atoms obtained from the MD-tar simulations in explicit water for the three glycopeptides; (b) number of water molecules of the first hydration shell (<2.8 Å from the solute heteroatoms) obtained from the MD-tar simulations in explicit water; (c) 2D radial pair distribution function of N1 and N5 and a representative frame of the MD-tar simulation of glycopeptide **1** showing a bridging water molecule. The maximum density of this shared water site was 1.6 times the bulk density, with maximum and average residence times of 6.0 and 0.5 ps, respectively.

Once the structure features were elucidated, the next step should be to try to deduce a possible structure–activity relationship. It is noteworthy to mention that the structure of the first hydration shell should play a pivotal role in defin-

ing the antifreeze activity of these molecules. Thus, we first decided to calculate the number of close neighbor water molecules as a function of time. The average hydration number was higher for molecule **1** than for its non-natural glycopeptide analogues, which indicates that both the rigidity and the extended conformation of the backbone favor better interaction with the first hydration shell (Figure 8b). Moreover, we investigated the anisotropic hydration of these molecules by calculating the normalized 2D radial pair distributions[24] for all possible shared water density sites between the sugar and peptide moieties. These 2D functions give the probability, $g(r1,r2)$, of finding a water molecule at a distances $r1$ and $r2$ from two selected solute atoms (oxygen and nitrogen atoms in our molecules), relative to the probability expected for a random distribution. Thus, if this probability is higher than the unit (bulk water density), then structural or semistructural water molecules are present between the two solute atoms that define the 2D function (Figure 8c).

The analysis of the MD-tar simulations in explicit water also revealed the existence of an interesting water bridge between NH1 and NH5 for compound **1** (Figure 8c). This finding is in agreement with the NOE observed between these two protons (Figure 3b, left panel) and also with the results previously obtained by our group for the simplest mucin-like glycopeptide model, derived from Thr.[19] Conversely, no relevant water-mediated interactions were found for derivatives **2** and **3**. These findings indicate that the orientation of the sugar moiety with respect to the peptide plays a key role in different events. It defines the flexibility of the underlying amino acids (backbone) and, probably more important within the antifreeze context, it permits (or not), the proper structure of the surrounding water molecules.

Conclusions

The synthesis and conformational analysis in aqueous solution of three antifreeze-like glycopeptides containing the sequence Xaa(α-GalNAc)-Ala-Ala, where Xaa is either threonine (Thr) or the non-natural amino acids α-methylserine (MeSer) or α-methylthreonine (MeThr), has been achieved. Notably, whereas the Thr derivative is rather rigid in solution and exhibits an extended conformation for the backbone, the non-natural glycopeptides are rather flexible, presenting a random coil conformation for the peptide sequence. For this reason, the Thr-containing glycopeptide is able to structure the surrounding water molecules, showing an interesting water pocket between the sugar and peptide backbone moieties. Thus, the orientation of the sugar moiety with respect to the peptide plays an important role in structuring the water molecules and in defining the flexibility of the underlying polypeptide backbone. Therefore, the different behaviors of these molecules in both dynamics and hydration properties make them suitable systems to shed light on the key factors that govern antifreeze activity.

Experimental Section

General Procedures: Solvents were purified according to standard procedures. Analytical TLC was performed by using Polychrom SI F254 plates. Column chromatography was performed by using silica gel 60 (230–400 mesh). ^{1}H and ^{13}C NMR spectra were recorded with Bruker ARX 300 and Bruker Avance 400 spectrometers. ^{1}H and ^{13}C NMR spectra were recorded in $CDCl_3$ or CD_3OD with TMS as the internal standard and in D_2O (chemical shifts are reported in ppm on the δ scale, coupling constants in Hz). Optical rotations were measured with a Perkin–Elmer 341 polarimeter. Microanalyses were carried out with a CE Instruments EA-1110 analyzer and are in good agreement with the calculated values. Preparative reverse-phase HPLC was performed by using a Phenomenex® column, Luna 10 μm C18(2) 100 Å, AXIA Packed 250 × 21.2 mm. Injection volume: 500 μL. Detector λ = 210 nm.

5: 3,4,6-Tri-*O*-benzyl-2-nitrogalactal (660 mg, 1.43 mmol) and MeSer derivative **4**[25] (400 mg, 1.71 mmol) were dissolved in THF (30 mL) under an argon atmosphere in the presence of molecular sieves. The reaction mixture was stirred at 25 °C for 30 min and a solution of potassium *tert*-butoxide (1 M in THF, 0.3 mL, 0.3 mmol) was then added. After the reaction was stirred for an additional 12 h, the molecular sieves were filtered off and all solvents were removed by evaporation. The residue was purified by a silica gel column chromatography (hexane/ethyl acetate, 4:1) to give **5** (660 mg, 67%) as a colorless oil. $[\alpha]_D^{25}$ = +63.6 (c = 1.1, $CHCl_3$). ^{1}H NMR (400 MHz, $CDCl_3$): δ = 1.32–1.40 (m, 12 H, Boc, Meα), 3.42–3.49 (m, 1 H, H6s), 3.50–3.57 (m, 1 H, H6s), 3.60 (d, J = 9.6 Hz, 1 H, Hβ), 3.67 (s, 3 H, CO_2Me), 3.87–3.95 (m, 1 H, H5s), 3.96–4.01 (m, 1 H, H4s), 4.11–4.24 (m, 1 H, Hβ), 4.26–4.35 (m, 2 H, 1 C*H*$_2$Ph, H3s), 4.35–4.44 (m, 2 H, 1 C*H*$_2$Ph), 4.59–4.67 (m, 2 H, 2 C*H*$_2$Ph), 4.74 (d, J = 11.1 Hz, 1 H, 1 C*H*$_2$Ph), 4.82–4.92 (m, 1 H, H2s), 5.12–5.20 (m, 1 H, H1s), 5.28 (s, 1 H, N*H*Boc), 7.10–7.29 (m, 15 H, Arom.) ppm. ^{13}C NMR (100 MHz, $CDCl_3$): δ = 20.6, 28.2, 52.8, 59.5, 67.7, 69.6, 70.1, 72.9, 73.5, 75.0, 75.1, 79.7, 84.2, 96.6, 127.8, 128.0, 128.1, 128.3, 128.4, 128.5, 137.3, 137.6, 137.9, 154.2, 172.8 ppm. $C_{37}H_{46}N_2O_{11}$ (694.78): calcd. C 63.96, H 6.67, N 4.03; found C 64.00, H 6.65, N 4.06.

6: Platinized Raney-nickel (T4) catalyst was freshly prepared as described in the literature.[26] The catalyst obtained by using 2.0 g of Raney nickel/aluminum alloy was suspended in ethanol (10 mL) and prehydrogenated for 10 min before the addition of **5** (119 mg, 0.17 mmol) in ethanol/ethyl acetate (4:1, 5 mL). The reaction mixture was shaken under an atmosphere of H_2 (1 atm) for 4 h at 25 °C. The catalyst was filtered off, and the solvent was evaporated. The residue was dissolved in pyridine/acetic anhydride (2:1, 6 mL) and stirred at 25 °C for 3 h. Removal of the volatiles and silica gel column chromatographic purification (ethyl acetate/hexane, 7:3) gave **6** (50 mg, 41%) as a colorless oil. $[\alpha]_D^{25}$ = +52.4 (c = 1.07, MeOH). ^{1}H NMR (400 MHz, CD_3OD): δ = 1.36 (s, 9 H, Boc), 1.38 (s, 3 H, Meα) 1.83 (s, 3 H, NH*Ac*), 3.46–3.57 (m, 4 H, Hβ, 2 H6s, H3s), 3.61 (s, 3 H, CO_2Me), 3.76–3.83 (m, 1 H, H5s), 3.84–3.90 (m, 1 H, Hβ), 3.91–3.94 (m, 1 H, H4s), 4.33–4.44 (m, 3 H, 3 C*H*$_2$Ph), 4.49 (d, J = 11.6 Hz, 1 H, 1 C*H*$_2$Ph), 4.53–4.59 (m, 1 H, H2s), 4.63 (d, J = 12.2 Hz, 1 H, 1 C*H*$_2$Ph), 4.77 (d, J = 3.6 Hz, 1 H, H1s), 4.86 (d, J = 11.6 Hz, 1 H, 1 C*H*$_2$Ph), 5.23 (s, 1 H, N*H*Boc), 5.42 (d, J = 8.8 Hz, 1 H, N*H*Ac), 7.18–7.29 (m, 15 H, Arom.) ppm. ^{13}C NMR (100 MHz, CD_3OD): δ = 23.2, 28.2, 28.3, 48.9, 52.5, 59.7, 68.6, 69.9, 71.2, 71.5, 72.5, 73.4, 74.4, 77.1, 98.8, 127.4, 127.7, 127.8, 127.8, 128.0, 128.1, 128.3, 128.4, 128.4, 137.9, 138.0, 138.5, 154.6, 169.8, 173.0 ppm. $C_{39}H_{50}N_2O_{10}$ (706.82): calcd. C 66.27, H 7.13, N 3.96; found C 66.30, H 7.15, N 4.00.

7: LiOH·H_2O (24 mg, 0.56 mmol) was added to a solution of **6** (80 mg, 0.11 mmol) in H_2O/MeOH (1:4, 10 mL). After the reaction mixture was stirred at 25 °C for 12 h, LiOH·H_2O (24 mg, 0.56 mmol) was added again, and stirring was maintained for an additional 12 h. The solvent was then evaporated, and the residue was taken up in diethyl ether (15 mL). The organic layer was washed with 1 N HCl (5 mL), dried, and concentrated in vacuo. Desired acid **7** was obtained as a pallid yellow oil (74 mg, 97%), which was then directly used for the next step. $[a]_D^{25}$ = +57.7 (c = 1.05, MeOH). ^{1}H NMR (400 MHz, CD_3OD): δ = 1.43 (s, 9 H, Boc), 1.45 (s, 3 H, Meα) 1.99 (s, 3 H, NH*Ac*), 3.52–3.63 (m, 2 H, 2 H6s), 3.69 (d, J = 9.5 Hz, 1 H, Hβ), 3.80 (d, J = 10.8 Hz, 1 H, H3s), 3.94–4.07 (m, 3 H, Hβ, H4s, H5s), 4.43 (d, J = 11.7 Hz, 1 H, 1 CH_2Ph), 4.46–4.60 (m, 4 H, 4 CH_2Ph), 4.71 (d, J = 11.6 Hz, 1 H, 1 CH_2Ph), 4.77–4.84 (m, 2 H, 2 CH_2Ph), 7.18–7.39 (m, 15 H, Arom.) ppm. ^{13}C NMR (100 MHz, CD_3OD): δ = 23.0, 28.9, 50.8, 60.7, 70.0, 71.0, 72.3, 73.2, 74.4, 74.8, 75.8, 78.9, 100.1, 128.6, 128.7, 128.8, 129.0, 129.2, 129.4, 139.5, 140.0, 140.1, 173.5, 177.1 ppm. $C_{38}H_{48}N_2O_{10}$ (692.80): calcd. C 65.88, H 6.98, N 4.04; found C 65.84, H 7.00, N 4.00.

9: A solution of acid **7** (70 mg, 0.10 mmol) in acetonitrile (10 mL) was treated with DIEA (0.08 mL, 0.51 mmol), amine **8** (29 mg, 0.10 mmol) as previously described by our group,[15b] and TBTU (42 mg, 0.13 mmol), under an inert atmosphere. The reaction mixture was stirred at 25 °C for 12 h and then evaporated to give a residue, which was purified by silica gel column chromatography (CH_2Cl_2/MeOH, 15:1) to obtain compound **9** (83 mg, 97%) as a colorless oil. $[a]_D^{25}$ = +52.1 (c = 1.02, MeOH). ^{1}H NMR (400 MHz, $CDCl_3$): δ = 1.30 (d, J = 7.3 Hz, 3 H, Me_{Ala}), 1.32–1.37 (m, 12 H, 9 Boc, Me_{Ala}), 1.38 (s, 3 H, Meα), 1.82 (s, 3 H, Me_S), 2.69 (d, J = 4.5 Hz, 3 H, Me_N), 3.40 (d, J = 10.0 Hz, 1 H, Hβ), 3.42–3.55 (m, 2 H, 2 H6s), 3.55–3.60 (m, 1 H, H3s), 3.65 (d, J = 10.1 Hz, 1 H, Hβ), 3.75 ("t", J = 6.5 Hz, 1 H, H5s), 3.93–4.01 (m, 1 H, H4s), 4.02–4.12 (m, 1 H, HαAla), 4.23–4.31 (m, 1 H, H2s), 4.31–4.44 (m, 4 H, 3 CH_2Ph, HαAla), 4.51 (d, J = 11.5 Hz, 1 H, 1 CH_2Ph), 4.66 (d, J = 12.0 Hz, 1 H, 1 CH_2Ph), 4.80 (d, J = 11.5 Hz, 1 H, 1 CH_2Ph), 5.16–5.24 (m, 1 H, H1s), 5.61–5.72 (m, 2 H, N*H*Boc, NH_{Sugar}), 6.80 (s, 1 H, N*H*Ac), 6.85 (d, J = 3.9 Hz, 1 H, NHAla), 7.15–7.35 (m, 15 H, Arom.), 7.57 (d, J = 7.7 Hz, 1 H, NHAla) ppm. ^{13}C NMR (100 MHz, $CDCl_3$): δ = 17.4, 18.8, 23.3, 26.2, 28.2, 49.1, 50.2, 51.0, 60.1, 68.5, 70.0, 71.2, 71.8, 72.5, 73.6, 74.5, 76.2, 81.2, 98.2, 127.7, 127.9, 128.0, 128.2, 128.3, 128.4, 128.7, 137.5, 137.6, 138.1, 155.6, 170.6, 171.9, 173.0, 173.1 ppm. $C_{45}H_{61}N_5O_{11}$ (847.99): calcd. C 63.74, H 7.25, N 8.26; found C 63.84, H 7.18, N 8.25.

10: TFA (3 mL) was added to a solution of compound **9** (50 mg, 0.06 mmol) in CH_2Cl_2 (3 mL) at 0 °C. The reaction was maintained at this temperature for 30 min, warmed at 25 °C for 3 h, and then concentrated. The crude was dissolved in pyridine/Ac_2O (2:1, 3 mL), and the mixture was stirred for 3 h at 25 °C. The solvent was evaporated, and the crude was purified by silica gel column chromatography (CH_2Cl_2/MeOH, 15:1) to give **10** (20 mg, 43%) as a colorless oil. $[a]_D^{25}$ = +57.3 (c = 1.09, MeOH). ^{1}H NMR (400 MHz, CD_3OD): δ = 1.34–1.42 (m, 6 H, Me2, Me1), 1.54 (s, 3 H, Meα), 1.98 (s, 3 H, Me_C), 1.99 (s, 3 H, Me_S), 2.74 (s, 3 H, Me_N), 3.47–3.61 (m, 3 H, H6s, Hβ), 3.74–3.83 (m, 2 H, H3s, H5s), 3.93 (d, J = 9.3 Hz, 1 H, Hβ), 3.97–4.00 (m, 1 H, H4s), 4.20 (q, J = 7.3 Hz, 1 H, HαAla), 4.30 (q, J = 7.3 Hz, 1 H, HαAla), 4.40 (d, J = 11.8 Hz, 1 H, 1 CH_2Ph), 4.44–4.52 (m, 2 H, 2 CH_2Ph), 4.56 (dd, J = 11.1, 3.5 Hz, 1 H, H2s), 4.61 (d, J = 11.7 Hz, 1 H, 1 CH_2Ph), 4.74 (d, J = 11.7 Hz, 1 H, 1 CH_2Ph), 4.79–4.85 (m, 2 H, 1 CH_2Ph, H1s), 7.21–7.41 (m, 15 H, Arom.) ppm. ^{13}C NMR (100 MHz, CD_3OD): δ = 17.3, 17.7, 20.8, 22.8, 23.2, 26.5, 50.7, 50.7, 52.1, 60.6, 70.1, 71.4, 72.7, 73.2, 74.5, 74.8, 75.8, 78.2, 99.7, 128.6, 128.8, 129.1, 129.2, 129.5, 139.3, 139.8, 140.0, 173.4, 173.5, 175.0, 175.6, 175.8 ppm. $C_{42}H_{55}N_5O_{10}$ (789.91): calcd. C 63.86, H 7.02, N 8.87; found C 63.84, H 7.08, N 8.85.

2: A solution of compound **10** (20 mg, 0.02 mmol) in MeOH/ethyl acetate (4:1, 5 mL) was treated with 10% Pd/C (15 mg) as a catalyst. The reaction mixture was shaken under an atmosphere of H_2 (1 atm) for 12 h at 25 °C. The catalyst and the solvent were removed, and the crude product was purified by preparative reverse-phase HPLC (flow rate 20 mL min^{-1}, t_R = 6.32 min) in CH_3CN/H_2O (2:98) to give **2** (13 mg) as a colorless oil in 95% yield. $[a]_D^{25}$ = +62.2 (c = 0.58, H_2O). ^{1}H NMR (400 MHz, D_2O): δ = 1.39 (br. s, 3 H, Me2), 1.41 (br. s, 3 H, Me1), 1.53 (s, 3 H, Meα), 2.04 (s, 3 H, Me_C), 2.07 (s, 3 H, Me_S), 2.76 (s, 3 H, Me_N), 3.73–3.95 (m, 6 H, 2 Hβ, 2 H6s, H5s, H3s), 3.98–4.02 (m, 1 H, H4s), 4.17 (dd, J = 11.1, 3.4 Hz, 1 H, H2s), 4.21–432 (m, 2 H, Hα2, Hα3), 4.90 (d, J = 3.3 Hz, 1 H, H1s) ppm. ^{1}H NMR (H_2O/D_2O): δ = 1.31–1.39 (m, 6 H), 1.48 (s, 3 H), 1.99 (s, 3 H), 2.03 (s, 3 H), 2.71 (d, J = 4.5 Hz, 3 H), 3.67–3.76 (m, 3 H), 3.76–3.82 (m, 1 H), 3.83–3.89 (m, 2 H), 3.93–3.98 (m, 1 H), 4.07–4.15 (m, 1 H), 4.16–4.26 (m, 2 H), 4.82 (br. s, 1 H), 7.68–7.76 (m, 1 H), 8.04 (d, J = 6.1 Hz, 1 H), 8.11 (d, J = 8.9 Hz, 1 H), 8.28 (d, J = 5.5 Hz, 1 H), 8.31 (s, 1 H) ppm. ^{13}C NMR (100 MHz, D_2O): δ = 16.2, 16.5, 20.2, 22.0, 22.2, 25.9, 49.8, 50.0, 50.1, 59.2, 61.2, 67.5, 68.4, 69.8, 71.3, 97.5, 173.9, 174.4, 174.8, 174.9, 175.3 ppm. $C_{21}H_{37}N_5O_{10}$ (519.55): calcd. C 48.55, H 7.18, N 13.48; found C 48.60, H 7.08, N 13.50.

NMR Experiments: NMR experiments were recorded with a Bruker Avance 400 spectrometer at 293 K. Magnitude-mode ge-2D COSY spectra were recorded with gradients and by using the cosygpqf pulse program with 90° pulse width. Phase-sensitive ge-2D HSQC spectra were recorded by using z-filter and selection before t1 removing the decoupling during acquisition by use of invigpndph pulse program with CNST2 (JHC) = 145. 2D NOESY experiments were made by using phase-sensitive ge-2D NOESY with WATERGATE for H_2O/D_2O (9:1) spectra. Selective ge-1D NOESY experiments were carried out by using the 1D-DPFGE NOE pulse sequence. NOEs intensities were normalized with respect to the diagonal peak at zero mixing time. Experimental NOEs were fitted to a double exponential function, $f(t) = p_0(e^{-p1t})(1 - e^{-p2t})$ with p_0, p_1, and p_2 being adjustable parameters.[17] The initial slope was determined from the first derivative at time t = 0, $f'(0) = p_0p_2$. From the initial slopes, inter-proton distances were obtained by employing the isolated spin pair approximation.

Molecular Dynamics Simulations: MD-tar simulations in explicit TIP3P[27] water were performed with AMBER[28] 6.0 (AMBER94), which was implemented with GLYCAM 04 parameters[29] to accurately simulate the conformational behavior of the sugar moiety. RESP atomic charges for **1**–**3** were derived by applying the RESP module of AMBER to the HF/6-31G(d) ESP calculated charges. NOE-derived distances were included as time-averaged distance constraints, and scalar coupling constants J as time-averaged coupling constraints. $A<r^{-6}>^{-1/6}$ average was used for the distances and a linear average was used for the coupling constants. Final trajectories were run by using an exponential decay constant of 1600 ps and a simulation length of 16 ns. $^3J_{H\alpha,H\beta}$ and $^3J_{NH,H\alpha}$ coupling constants were estimated by using the Karplus equations given in the bibliography.[30]

Supporting Information (see footnote on the first page of this article): Experimental procedures and characterization data; results of the MD simulations and HPLC chromatograms.

Acknowledgments

We are grateful to the Ministerio de Educación y Ciencia (project CTQ2009-13814/BQU, grant to A. F.-T.), Gobierno de La Rioja (Colabora 2007/18), and the Universidad de La Rioja (project EGI09/60, grant to M. G.-L.). F. R. thanks the CSIC for his JAE-Doc Program contract. We also thank CESGA for computer support.

[1] a) M. M. Harding, P. I. Anderberg, A. D. Haymet, *Eur. J. Biochem.* **2003**, *270*, 1381–1392; b) Y. Yeh, R. E. Feeney, *Chem. Rev.* **1996**, *96*, 601–617; c) R. E. Feeney, T. S. Burcham, Y. Yeh, *Annu. Rev. Biophys. Biophys. Chem.* **1986**, *15*, 59–78; d) G. L. Fletcher, C. L. Hew, P. L. Davies, *Annu. Rev. Physiol.* **2001**, *63*, 359–390.

[2] F. Tablin, A. E. Oliver, N. J. Walker, L. M. Crowe, J. H. Crowe, *J. Cell Physiol.* **1996**, *168*, 305–313.

[3] J. H. Wang, *Cryobiology* **2000**, *41*, 1–9.

[4] R. E. Feeney, Y. Yeh, *Trends Food Sci. Technol.* **1998**, *9*, 102–106.

[5] Y. Tachibana, G. L. Fletcher, N. Fujitani, S. Tsuda, K. Monde, S. I. Nishimura, *Angew. Chem. Int. Ed.* **2004**, *43*, 856–862.

[6] C. Heggemann, C. Budke, B. Schomburg, Z. Majer, M. Wibbrock, T. Koop, N. Sewald, *Amino Acids* **2010**, *38*, 213–222.

[7] A. Masuda, T. Baba, N. Dohmae, M. Yamamura, H. Wada, K. Ushida, *J. Nat. Prod.* **2007**, *70*, 1089–1092.

[8] a) C. A. Bush, R. E. Feeney, *Int. J. Pept. Protein Res.* **1986**, *28*, 386–397; b) A. N. Lane, L. M. Hays, R. E. Feeney, L. M. Crowe, J. H. Crowe, *Protein Sci.* **1998**, *7*, 1555–1563.

[9] Y. Uda, S. Zepeda, F. Kaneko, Y. Matsuura, Y. Furukawa, *J. Phys. Chem. B* **2007**, *111*,14355–14361.

[10] a) S. Liu, R. N. Ben, *Org. Lett.* **2005**, *7*, 2385–2388; b) R. Y. Tam, C. N. Rowley, I. Petrov, T. Zhang, N. A. Afagh, T. K. Woo, R. N. Ben, *J. Am. Chem. Soc.* **2009**, *131*, 15745–15753.

[11] P. Czechura, R. Y. Tam, E. Dimitrijevic, A. V. Murphy, R. N. Ben, *J. Am. Chem. Soc.* **2008**, *130*, 2928–2929.

[12] J. Garner, K. A. Jolliffe, M. M. Harding, R. J. Payne, *Chem. Commun.* **2009**, 6925–6927.

[13] a) C. Cativiela, M. D. Díaz-de-Villegas, *Tetrahedron: Asymmetry* **1998**, *9*, 3517–3599; b) C. Cativiela, M. D. Díaz-de-Villegas, *Tetrahedron: Asymmetry* **2000**, *11*, 645–732; c) C. Cativiela, M. D. Díaz-de-Villegas, *Tetrahedron: Asymmetry* **2007**, *18*, 569–623; d) H. Vogt, S. Bräse, *Org. Biomol. Chem.* **2007**, *5*, 406–430.

[14] a) A. Moretto, F. Formaggio, M. Crisma, C. Toniolo, M. Saviano, R. Iacovino, R. M. Vitale, E. Benedetti, *J. Pept. Res.* **2001**, *57*, 307–315; b) R. Gessmann, H. Bruckner, K. Petratos, *J. Pept. Sci.* **2003**, *9*, 753–762; c) M. Crisma, A. Moretto, M. Rainaldi, F. Formaggio, Q. B. Broxterman, B. Kaptein, C. Toniolo, *J. Pept. Sci.* **2003**, *9*, 620–637.

[15] a) A. Fernández-Tejada, F. Corzana, J. H. Busto, A. Avenoza, J. M. Peregrina, *J. Org. Chem.* **2009**, *74*, 9305–9313; b) A. Fernández-Tejada, F. Corzana, J. H. Busto, A. Avenoza, J. M. Peregrina, *Org. Biomol. Chem.* **2009**, *7*, 2885–2893; c) A. Fernández-Tejada, F. Corzana, J. H. Busto, G. Jiménez-Osés, J. Jiménez-Barbero, A. Avenoza, J. M. Peregrina, *Chem. Eur. J.* **2009**, *15*, 7297–7301; d) A. Fernández-Tejada, F. Corzana, J. H. Busto, G. Jiménez-Osés, J. M. Peregrina, A. Avenoza, *Chem. Eur. J.* **2008**, *14*, 7042–7058.

[16] a) G. A. Winterfeld, Y. Ito, T. Ogawa, R. R. Schmidt, *Eur. J. Org. Chem.* **1999**, 1167–1171; b) G. A. Winterfeld, R. R. Schmidt, *Angew. Chem.* **2001**, *113*, 2718–2721; *Angew. Chem. Int. Ed.* **2001**, *40*, 2654–2657; c) R. R. Schmidt, Y. D. Vankar, *Acc. Chem. Res.* **2008**, *41*,1059–1073.

[17] T. Haselhorst, T. Weimar, T. Peters, *J. Am. Chem. Soc.* **2001**, *123*, 10705–10714.

[18] H. J. Dyson, P. E. Wright, *Annu. Rev. Biophys. Biophys. Chem.* **1991**, *20*, 519–538.

[19] F. Corzana, J. H. Busto, G. Jiménez-Osés, M. García de Luis, J. L. Asensio, J. Jiménez-Barbero, J. M. Peregrina, A. Avenoza, *J. Am. Chem. Soc.* **2007**, *129*, 9458–9467.

[20] a) D. A. Pearlman, *J. Biomol. NMR* **1994**, *4*, 279–299; b) A. E. Torda, R. M. Brunne, T. Huber, H. Kessler, W. F. van Gunsteren, *J. Biomol. NMR* **1993**, *3*, 55–66.

[21] L. Kindahl, C. Sandstorm, A. G. Craig, T. Norberg, L. Kenne, *Can. J. Chem.* **2002**, *80*, 1022–1031.

[22] G. R. J. Thatcher, *The Anomeric Effect and Associated Stereoelectronic Effects*, ACS, Washington, **1993**.

[23] F. Corzana, J. H. Busto, G. Jiménez-Osés, J. L. Asensio, J. Jiménez-Barbero, J. M. Peregrina, A. Avenoza, *J. Am. Chem. Soc.* **2006**, *128*, 14640–14648.

[24] C. Andersson, S. B. Engelsen, *J. Mol. Graphics* **1999**, *17*, 101–105.

[25] A. Avenoza, C. Cativiela, F. Corzana, J. M. Peregrina, D. Sucunza, M. M. Zurbano, *Tetrahedron: Asymmetry* **2001**, *12*, 949–957.

[26] S. Nishimura, *Bull. Chem. Soc. Jpn.* **1959**, *32*, 61–64.

[27] M. W. Mahoney, W. L. Jorgensen, *J. Chem. Phys.* **2000**, *112*, 8910–8922.

[28] D. A. Case, D. A. Pearlman, J. W. Caldwell, T. E. Cheatham III, W. S. Ross, C. L. Simmerling, T. A. Darden, K. M. Merz, R. V. Stanton, A. L. Cheng, J. J. Vincent, M. Crowley, V. Tsui, R. J. Radmer, Y. Duan, J. Pitera, I. Massova, G. L. Seibel, U. C. Singh, P. K. Weiner, P. A. Kollman, *AMBER 6*, University of California, San Francisco, **1999**.

[29] R. J. Woods, R. A. Dwek, C. J. Edge, B. Fraser-Reid, *J. Phys. Chem.* **1995**, *99*, 3832–3846.

[30] a) A. Marco, M. Llinas, K. Wuthrich, *Biopolymers* **1978**, *17*, 617–636; b) G. W. Vuister, A. Bax, *J. Am. Chem. Soc.* **1993**, *115*, 7772–7777.

Received: March 18, 2010
Published Online: May 12, 2010

